

Dynamically regulated star formation in the strongly interacting Taffy galaxies

Axel García-Rodríguez^{1,*}, Antonio Usero^{1,**}, Santiago García-Burillo¹, Frank Bigiel², Elias Brinks³, Asunción Fuente¹, Adam K. Leroy⁴, and Miguel Querejeta¹

¹Observatorio Astronómico Nacional (IGN), C/ Alfonso XII, 3, Madrid 28014, Spain

²Argelander-Institut für Astronomie, Universität Bonn, Auf dem Hügel 71, 53121 Bonn, Germany

³Centre for Astrophysics Research, University of Hertfordshire, Hatfield AL10 9AB, UK

⁴Department of Astronomy, The Ohio State University, 140 West 18th Ave, Columbus, OH 43210, USA

Abstract. The Taffy system stands out as one of the strongest gas-rich galaxy mergers with little star formation (SF) activity. We study the causes of this SF inefficiency by observing with the IRAM 30m telescope the line emission of several species in 6 positions. We report clear detections of tracers of bulk (^{12}CO and ^{13}CO) and dense (HCN and HCO^+) molecular gas in all regions, as well as evidence for shocks ($\text{SiO } J=2-1$) over the intergalactic bridge. Our observations not only confirm the SF inefficiency of the bulk gas, but they also show that the SF efficiency of the dense gas phase is abnormally low too (~ 1 dex below ULIRGs). The dense gas fraction ($\propto \text{HCN}/\text{CO}$) only shows small variations across the entire system, with a typical value of 4%. Although this fraction is somewhat low compared to other interacting/merging systems, it is similar to the values measured in the disk of nearby, normal star-forming galaxies. Finally, we use the outstanding properties of the Taffy system to place constraints on some of the turbulence-regulated SF models from the literature.

1 Introduction

The Taffy system was formed ~ 23 Myr ago after the high-speed, head-on collision of the galaxy pair UGC 12914/5 [1]. This strong interaction has created a 20 kpc-long massive and turbulent intergalactic bridge of atomic and molecular gas [1–3]. The mass of molecular gas in the bridge ($\sim 2 \times 10^9 M_{\odot}$) is similar to that of the entire Milky Way. However, unlike in other gas-rich interacting/merging systems [4], the star formation (SF) in Taffy is not enhanced but rather inhibited [5–7]. The Taffy system is thus an ideal testbed for understanding SF in violent environments. In particular, it is interesting to understand which mechanisms are hindering the SF in Taffy despite having perfect conditions to trigger strong starburst events.

2 Observations

We carried out line observations at 3 mm using the IRAM-30m radiotelescope. Specifically, we selected 6 representative pointings that cover the main environments (see Figure 1 – left),

*e-mail: axel.garcia@oan.es

**e-mail: a.usero@oan.es

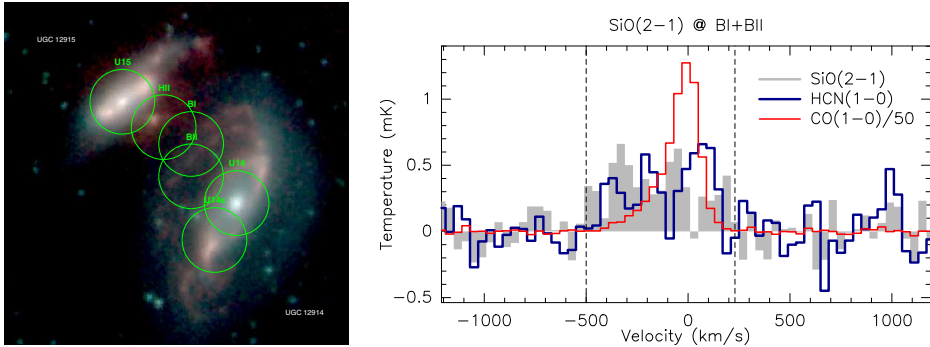


Figure 1. *Left:* IRAM-30m pointings (green circles) overlaid on an archival RGB image of Taffy from IRAC (R: 5.7 μ m; G: 4.5 μ m; B: 3.6 μ m). The size of the circles is 28'' (\sim 8.3 kpc), which corresponds to the beam size of the IRAM-30m at \sim 90 GHz. *Right:* SiO(2–1) combined spectrum from regions BI and BII. Re-scaled versions of CO(1–0) and HCN(1–0) spectra are superimposed in red and blue.

including both galaxy centers (U14 and U15 in Figure 1). The extragalactic H α region (HIII), which is the only spot within the bridge with intense SF, was also observed to compare it with the other two bridge position (BI and BII; Figure 1). We successfully detected several tracers of bulk molecular gas (e.g., $^{12}\text{CO}(1-0)$, $^{13}\text{CO}(1-0)$), dense gas (e.g., HCN(1–0), $\text{HCO}^+(1-0)$), and even shocks (SiO(2–1); see Figure 1–right). The data reduction process of all these molecular lines has followed a standard procedure similar to that adopted by [8].

3 Causes of the SF inefficiency

According to previous works, the star formation efficiency ($\text{SFE} \propto \text{SFR}/\text{CO}$) of the Taffy system is considerably lower than that of other highly interacting systems like ULIRGS [5–7]. We confirm this behaviour using CO(1–0) as mass tracer, and GALEX far-UV + MIPS 24 μ m as a hybrid star formation rate (SFR) indicator. We see that the SFE of all our bridge observations fall roughly a factor 4–8 below the disk pointings (cyan circles and squares in Figure 3). These disk environments, in turn, are in good agreement with the efficiencies found in nearby Star-Forming Galaxies (SFG) [8], and \sim 1 dex below the SFE of ULIRGs [9]. In general, the SFE can be expressed as a product of two different factors: the dense gas fraction ($f_{\text{dense}} \propto \text{HCN}/\text{CO}$) and the star formation efficiency of the dense gas ($\text{SFE}_{\text{dense}} \propto \text{SFR}/\text{HCN}$). A decrease in any of them could explain why the SFE of Taffy is depressed. Figure 2 left and right represent, respectively, our estimations for f_{dense} and $\text{SFE}_{\text{dense}}$ (derived as in [8]) against the stellar surface density (Σ_{star}). For comparison purposes, we have also added as black points the sample of SFG from [8], and, as orange bands, we show the fitted trends for the EMPIRE galaxies [10].

Dense gas fractions (coloured points in Fig. 2–left) appear to be quite homogeneous across Taffy, with a typical value of \sim 4%. This fraction is compatible with the low-end value of the SFG sample, making all Taffy environments consistent with the overall trend followed by SFG. In comparison, f_{dense} is systematically higher in ULIRGs, reaching typical values of 20% [9]. To certain degree, these results suggest that at least part of the SF inefficiency found in Taffy can be interpreted as a lack of dense gas within the system.

In contrast, the right-hand panel of Fig. 2 shows very different results. The $\text{SFE}_{\text{dense}}$ of the Taffy system presents nearly the opposite behaviour than the trends followed by both SFG samples. In fact, although the disk environments in Taffy remain comparable to other SFGs,

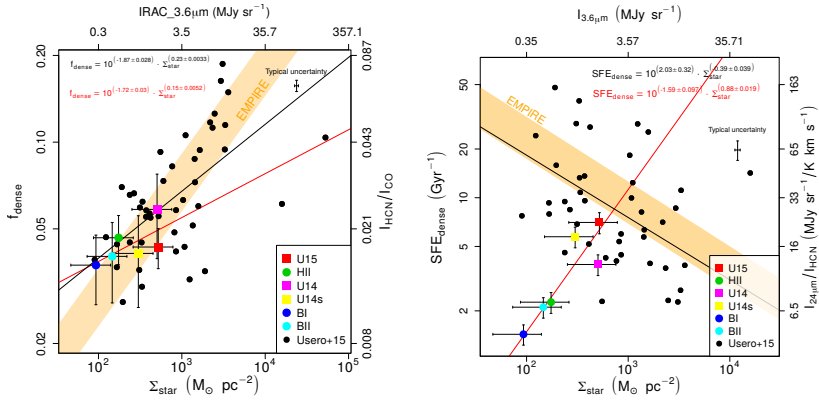


Figure 2. Dense gas fraction (left) and star formation efficiency of the dense gas (right) as a function of the stellar surface density. Coloured points represent our Taffy observations, whereas the black ones stand for different SFG [8] or (U)LIRGs [9]. Orange bands show the fitted trend and scatter of the EMPIRE galaxies [10] in the same parameter space. Within the Taffy sample, squares illustrate the galactic pointings, while circles show the extragalactic ones. Finally, the black and red lines correspond, respectively, to the fitted deming regression model to the SFG sample and to the Taffy sample.

all bridge pointings show extremely low SFE_{dense} for their corresponding Σ_{star} . Indeed, these regions have ~ 1 dex lower SFE_{dense} than expected from the EMPIRE sample (orange band). Altogether, we conclude there exists a global lack of dense gas in Taffy compared to other highly interacting systems. However, the relative contrast in the SF activity of both galaxy disks and that of the intergalactic bridge can only be explained by an unusually low SFE_{dense} .

We propose that the enhanced level of turbulence in the bridge [3, 11, 12] lowers the SFE_{dense} in this region. In this regard, we report the first detection of SiO(2–1) in this system. The SiO line, one of the most reliable shocks tracers, likely signposts strong cloud-cloud collisions. In Figure 1–right, we show the average SiO(2–1) spectrum in BI and BII, which are the pointings with the lowest SFR. We postulate that this SiO detection is an indirect evidence of an enhanced turbulence likely driven by the undergoing galaxy interaction.

4 Multi-free-fall SF models cannot explain observations

We can compare our observations with the predictions from the family of turbulence-regulated SF models [13]. Our Taffy sample complements other single-dish surveys of SFGs [8] or (U)LIRGs [9]. In general, these SF models differ in their assumptions about the density for SF onset, the density PDF, and the multi free-fall factor (multi-ff). The latter basically determines the rate of collapse of each density layer. In the end, the main free parameters are: the mean of the density PDF (\bar{n}), the virial parameter (α_{vir}), and the Mach number (\mathcal{M}). The coloured regions of Fig. 3 show the SFE_{dense} pairs predicted by the models over a generous range of conditions. Most models show very narrow ranges in SFE compared to the scatter in the observations. In fact, only the KM05 model [13], which is the only one with a fixed multi-ff=1, is able to encompass the broad empirical range in SFE.

5 Summary and conclusions

We have studied the dense molecular gas in the highly interacting Taffy system, finding that its low SFE is mainly attributed to both a lack of dense gas and a low SF efficiency of this

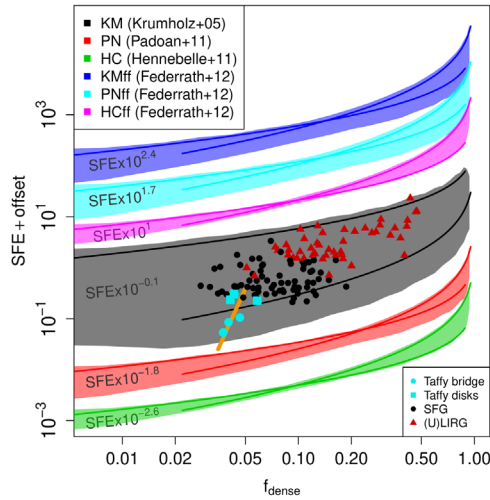


Figure 3. Comparison of different turbulence-regulated SF models with IRAM-30m observations (Taffy, SFG [8], (U)LIRGs [9]). Each coloured region represents the model predictions assuming $\bar{n} \in [10^0, 10^5] \text{ cm}^{-3}$, $\alpha_{vir} \in [0.8, 15]$, and $\mathcal{M} \in [10, 150]$. Each region is arbitrarily offset for the sake of visualisation. The colored curves correspond to minimum and maximum Mach numbers (10 and 150) for a fiducial virial parameter $\alpha_{vir} = 1.3$. The orange line is a linear fit to the Taffy data.

dense gas. Nevertheless, the relative difference in the SF activity between the galaxy disks and the intergalactic bridge can only be explained by a significantly lower $\text{SFE}_{\text{dense}}$ in the latter. Our detection of SiO supports the hypothesis that an enhanced turbulence is hindering the SF in the bridge. Finally, we combine our Taffy observations with literature data to place constraints on the family of turbulence-regulated SF models. Models with non-unity multi-ff [13] have problems to account for the observed scatter in the $\text{SFE} - f_{\text{dense}}$ parameter space.

References

- [1] Gao, Y., Zhu, M. & Seaquist, E. R., *AJ* **126**, 2171G (2003)
- [2] Braine, J., Davoust, E., Zhu, M. et al., *A&A* **516**, A40 (2003)
- [3] Vollmer, B., Braine, J. & Soida, M., *A&A* **547**, A39 (2012)
- [4] Genzel, R.; Tacconi, L. J.; Gracia-Carpio, J. et al., *MNRAS* **407**, 2091G (2010)
- [5] Peterson, B. W., Appleton, P. N., Bitsakis, T., et al., *ApJ* **855**, 141P (2018)
- [6] Joshi, B. A., Appleton, P. N., Blanc, G. A., et al., *ApJ* **878**, 161J (2019)
- [7] Appleton, P. N., Lanz, L., Bitsakis, T. et al., *ApJ* **812**, 118A (2015)
- [8] Usero, A., Leroy, A. K., Walter, F., et al., *AJ* **150**, 115 (2015)
- [9] García-Burillo, S., Usero, A., Alonso-Herrero, A. et al., *A&A* **539**, A8 (2012)
- [10] Jiménez-Donaire, M. J., Bigiel, F., Leroy, A. K. et al., *ApJ* **880**, 127J (2019)
- [11] Vollmer, B., Braine, J., Mazzilli-Ciraulo, B. et al., *A&A* **647**, A138 (2021)
- [12] Appleton, P. N. ; Emonts, B. ; Lisenfeld, U. et al., *ApJ* **931**, 121A (2022)
- [13] Federrath, C., and Klessen, R. S., *ApJ* **606**, 156 (2012)